Biochemistry Nanosensor Based on Hybrid Metallic Nanostructure Array

Shaoli Zhu, Chunlei Du*, Fei Li, Qileng Deng, Xiangang Luo**
State Key Laboratory of Optical Technologies for Microfabrication, Institute of Optics and Electronics,Chinese Academy of Sciences, Chengdu ,Sichuan Province, China 610209
*cldu@ioe.ac.cn and **lxg@ioe.ac.cn

ABSTRACT

A biochemistry nanosensor based on hybrid metallic nanostructure array was put forward in this paper. The hybrid metallic nanostructure array consists of two types Ag nanostuctures, spherical and pyramidal structures with the same period. A biochemistry sensor experiment is demonstrated by detecting the transmittance spectra of hybrid metallic nanostructure using Sciencetech spectrophotometer. The wave peaks of transmittance spectra have shifts when the metallic periods and the refractive index of Ag nanostuctures are different.

Keywords: hybrid nanostuctures, transmission, nanosensor, LSPR

1. INTRODUCTION

Biochemistry nanosensor is an active research topic in both life sciences and engineering[1]. It involves the interdisciplinary areas of life sciences and information sciences with bioinformatics, biochemistrychip, biocybernetics, bionics, and biocomputer. Their common characteristics are exploring and opening out the basic rules of the production, storage, transmission, process, transition, and control of the information in the biological systems, and discussing the basic methods which are employed for the human economy activity. The biosensor related research focuses on combination of the sensors and the diversified biological active materials as well as their relevant applications.

The localized surface plasmon resonance (LSPR) nanosensor becomes the hotspot problem because they have benign development situation and important position in the life sciences research[2-6]. LSPR nanosensor can be implemented using extremely simple, small, light, robust, low cost equipment. It has many traits such as convenience, high sensitivity, wide application and real-time detection etc. So it is deemed to be a kind of furthest potential biosensor.

The metal nanoparticles' optical properties mainly depend on their size, shape, metal composition and the refractive index of the surroundings. Previous research has shown that the localized surface plasmon resonance (LSPR) nanosensor, is a refractive index-based sensing device which relies on the extraordinary optical properties of noble (e.g., Ag, Au and Cu) metal nanoparticles[6-10]. The Ag nanoparticles have endowed the device with an excellent optical character. Especially, the peak of transmittance spectrumλ_{max} is unexpectedly sensitive to the nanoparticle's size, shape, and local external dielectric environment. Its sensitivity to the nanoenvironment has given us the fundament to develop a new serial of nanoscale affinity biochemosensors.

2. DESIGN THEORY OF THE BIOCHEMISTRY NANOSENSOR

A local surface plasma wave (LSPW) will be excited when the incident photon frequency is resonant with the collective oscillation of the conduction electrons and is known as the LSPR. The LSPR spectrum is the connection curve between the incident wavelength and the transmittance. The LSPR spectrum peaks are sensitive to the electric mediums on the surface of metal. Using this characteristic, we can fabricate the LSPR-based biosensor. The characteristic and functioning mechanism of our LSPR biochemosensor is that using a layer of inorganic pastern to change the refractive index of the medium surrounding the nanostuctures. We measured the variation of the refractive index of the medium so as to know the effect on the optical property of the nanosensor. Our design is that using two Ag layers for the symmetric nanostructure. The two layers have the same period but different height and shape. One is the pyramidal Ag particles

Holography and Diffractive Optics III, edited by Yunlong Sheng, Dahsiung Hsu, Chongxiu Yu
Proc. of SPIE Vol. 6832, 68320H, (2007) · 0277-786X/07/$18 · doi: 10.1117/12.757653

hexagonal distributed on the glass substrates, and the other is the spherical calotte Ag particles triangularly distributed on the glass substrates. We call it hybrid Ag nanostuctures hereinafter. Normally, there is only a layer of pyramidal silver structure distributed hexagonally on the glass substrates, as shown in Fig. 1. Our structure is a hybrid structure ombining the silver spherical calotte with the pyramidal particles together instead of the conventional Ag nanostuctures only. It cannot only produce the LSPR wave with the enlarged areal density of the Ag nanostuctures, but also couple and odulate the LSPR wave between the pyramidal Ag particles and the spherical Ag particles. The coupling in vertical direction acts as a resonant cavity in this case. Theoretically, it is synthesis of the interaction of the in-plane (horizontal) small pyramidal particles and the out-of-plane (vertical) coupling.

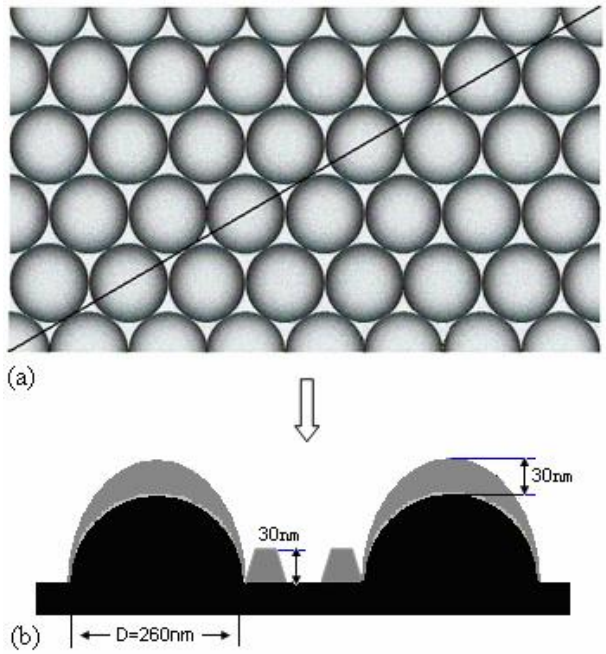

Fig. 1.(Color online) Schematic diagram of the Ag nanostuctures. (a) Top view of the particles; (b) cross-section view along diagonal direction with dimension of the spherical and pyramidal particles.

According to the structure model shown in Fig. 1(b), this type of net-distributed Ag particles can excite the LSPR. The hexagonal distributed microstructures can also excite the LSPR. The design theory was proposed in our previous work and the result is shown in Eq. (1)[11]

$$\lambda = \Lambda real\sqrt{\frac{\varepsilon_m \varepsilon_d}{\varepsilon_m + \varepsilon_d}} = \Lambda real\sqrt{\frac{n_m^{\ 2} n_d^{\ 2}}{n_m^{\ 2} + n_d^{\ 2}}} \tag{1}$$

2.1 Different periods of the nanostuctures array

In Eq. (1), for air n_d =1 , for Ag nanostuctures with different periods, Λ=260nm , Λ=300nm , and Λ=400nm. Left side of the equation is function of wavelength, and the right part n_m is relevant to the incident wavelength λ. Thus this is a transcendental equation. Its numerical solution can be derived from plotting. Crossing point of plotting for the left and right parts of the equation is the position of the LSPR resonant peak, as shown in Fig.2.

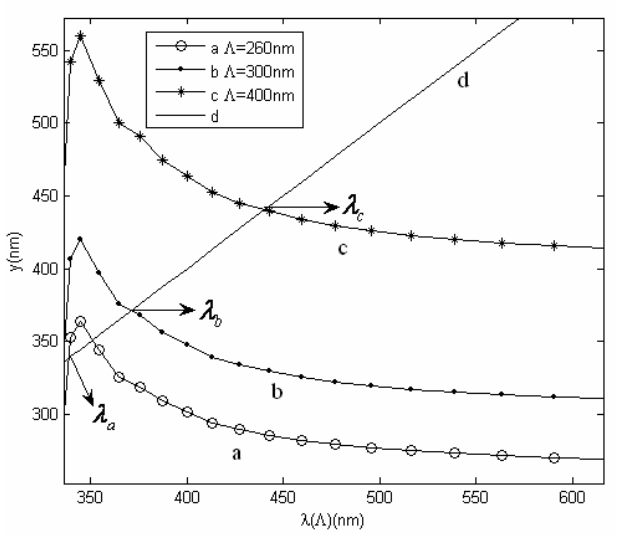

Fig.2 Curves obtained from solving the transcendental Eq. (1) of different periods. The resonant peak position is derived by plotting the two left and right parts of the equation for the crossing point.

In Fig.2, the curves a, b, and c can be expressed as $y = \Lambda real\sqrt{\frac{n_m^2 n_d^2}{n_m^2 + n_d^2}}$, n_d =1 , Λ=260nm , Λ=300nm , and Λ=400nm corresponds to the curves a, b, and c , respectively. d line expression is y=λ. It can be known from the crossing point that the position of resonant peak for the cases of Λ=260nm, Λ=300nm, and Λ=400nm is λ_a=338.4 nm, λ_b=371.14 nm, and λ_c=440.26 nm, respectively.

2.2 Different refractive index materials around the Ag nanostuctures

In Eq. (1), for air n_d =1 , for polymers with different refraction index, n_d =1.5 and 1.7. Left side of the equation is function of wavelength, and the right part n_m is relevant to the incident wavelength λ. Thus this is a transcendental equation. Its numerical solution can be derived from plotting. Crossing point of plotting for the left and right parts of the equation is the position of the LSPR resonant peak, as shown in Fig.3.

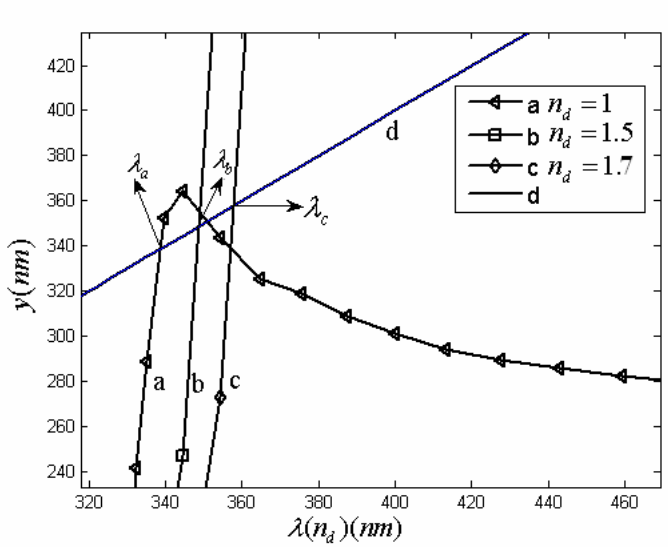

Fig.3 Curves obtained from solving the transcendental Eq. (1) of different refractive index materials around the Ag nanostuctures. The resonant peak position is derived by plotting the two left and right parts of the equation for the crossing point.

In Fig.3, the curves a, b, and c can be expressed as $y = \Lambda real\sqrt{\frac{n_m^2 n_d^2}{n_m^2 + n_d^2}}$, n_d =1, 1.5, and 1.7 corresponds to the curves a, b, and c , respectively. d line expression is y=λ. It can be known from the crossing point that the position of resonant peak for the cases of n_d =1, 1.5, and 1.7 is λ_a=338.4 nm, λ_b=348.5 nm, and λ_c=364.8 nm, respectively.

3. EXPERIMENTAL AND METHODS

3.1 Fabrication

Micronanofabracation technology was used to create surface-confined hybrid Ag nanostructures supported on a glass substrate. At first, the glass substrate was cleaned, and then the self-assembly of size-monodisperse nanospheres and were applied to form a deposition mask, followed by carving some microstructures on the glass substrate. After the removal of nanospheres by sonication in absolute ethanol for 3 min., Ag metal was deposited through the nanosphere masks using thermal or electron beam evaporation. By altering the nanosphere diameter and the deposited metal thickness, nanostructures with different in-plane width, out-of-plane height and interstructure space can be adjusted.

One of the surface modality of the samples was measured using atomic force microscopy (AFM) as shown in Fig. 4. The results show that in-plane width is ~260 nm and out-of-plane height is ~290 nm for the spherical calotte Ag particles; in-plane width is ~100 nm and out-of-plane height is ~30 nm for the pyramidal Ag nanostuctures. They have different shapes, period and height. These samples were coated with 30 nm thickness of Ag film. They are measured under the normal room temperature.

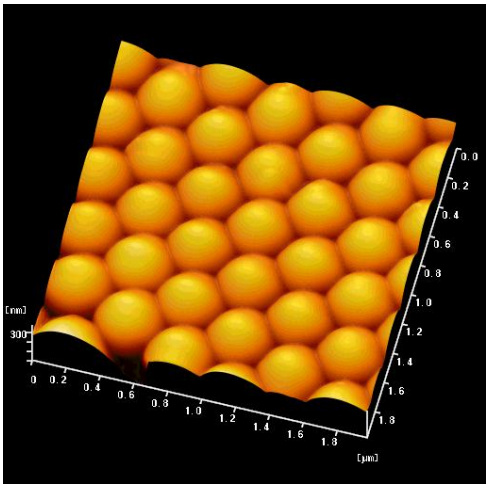

Fig.4 (Color online) The surface topography of hybrid metallic nanostuctures taken by an atomic force microscope (AFM).

3.2 Experimental setup

The transmittance spectrum of the chemosensors were measured by a scanning UV-visible-IR spectrophotometer. Figure 5 shows a schematic diagram of this experimental setup. UV-visible-IR transmittance spectrum was employed using white light which transmitted through a multimode optical fiber. The light exiting from the source with fiber coupler is focused onto the sample using a diaphragm and a collimating lens. The light transmitted through the sample was collected with an identical focus lens which is attached to the multimode fiber. A charge-coupled device (CCD) camera was connected with the multimode fiber and personal computer. The transmittance spectrum curve is directly shown on the screen of the computer. There are three steps for the measurement: the first step was to confirm the scale of the incident wavelength, which is ranging from 300 to 800 nm; and adjust the UV-visible-IR transmittance; second, to scan the background optics without samples in the sample holder; and last, to put the sample to the holder and scan, the samples vertical to the incident optics. Using an UV-visible-IR spectrophotometer can make the test simple, because the transmittance spectra were directly shown on the screen of the computer, there is no need for further data treatment.

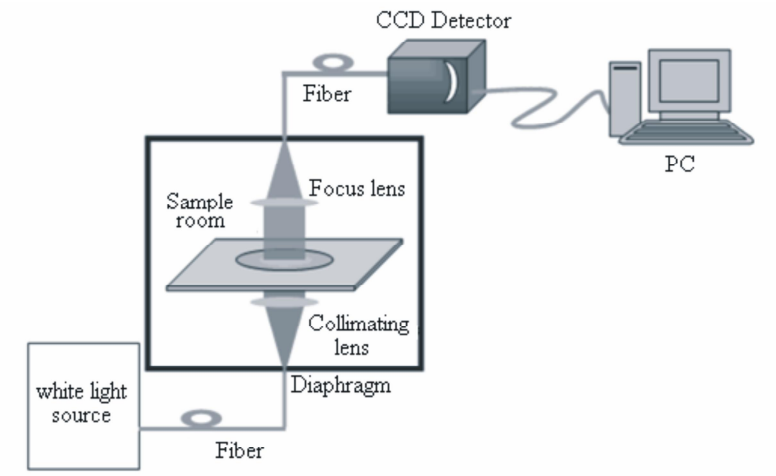

Fig.5 Schematic diagram of the scanning UV-visible-IR spectrophotometer used for measurement of the transmittance of the Ag nanostuctures.

Microscopic exhibition shows the existence of two wave peaks in the transmittance spectrum. One is the conventional wide peaks of the spectrum, and the other is the narrow parts of the spectrum. The uniqueness of our structure presents two aspects: first, there are two layers of Ag nanostuctures, both of them can produce the LSPR wave, in which they couple each other and generate a smooth transmittance line; the other is that this nanostructure can be used as the substrate for biological samples, the biological molecules can be easily connected with the structure, and the detective efficiency can be highly improved accordingly. Therefore, it can be employed to improve the sensitivity of the nanobiosensor.

In the different period experiments, different Ag nanostuctures periods were adjusted by the nanospheres' diameters of 260nm, 300nm, and 400nm, respectively. Using them can analyze the relationship between the Ag nanostuctures periods and the shift of the transmission spectrum.

In the sensing experiments, a type of inorganic pastern (comprise silicic and titanic oxide sol) was coated on the metal with pastern's refractive indices of 1.5 and 1.7, respectively. Then it forms a type of chemosensors which is sensitive to the index change of the Ag nanostuctures.

4. RESULTS AND DISCUSSIONS

4.1 Different Periods of the Ag nanostuctures array

The characteristics of the different Ag nanostuctures periods were carry through measuring their transmittance spectrum. In this experiment, the LSPR resonant peak of the Ag nanostuctures was also monitored when the Ag nanostuctures have different perieds (see Fig.6). First max value λ_{maxa} of the Ag nanostuctures was measured to be 388.08nm forΛ=260nm (see Fig.6 curve a). Then the period of Ag nanostucture is changed to Λ=300nm. The max value λ_{maxb} (see Fig.6 curve b) was measured to be 443.98nm, corresponding to an additional 55.9 nm red-shift; hereinafter, the sign "+" represents a redshift and the sign "-" for a blueshift, with respect to the Ag nanostuctures.. When the period of Ag nanostucture is changed to Λ=400nm, the max value λ_{maxc} (see Fig.6 curve c) was measured to be 542.09nm, corresponding to a +98.11nm shift. Moreover, the LSPR resonant peaks (also called absorption peaks) are denoted by λ_a', λ_b' and λ_c' which are 338.22nm, 372.97nm and 444.05nm respectively. It should be noted that different periods of the Ag nanostuctures have produced the different transmittance spectrum shifts. The larger of the periods of the Ag nanostuctures, the larger peak transmission shift and bandwidth of the LSPR spectrum is, as shown in Fig.6. This effect of enhancing the plasmon absorption by using different periods of the Ag nanostuctures can be used as immersion spectroscopy[12] for future use.

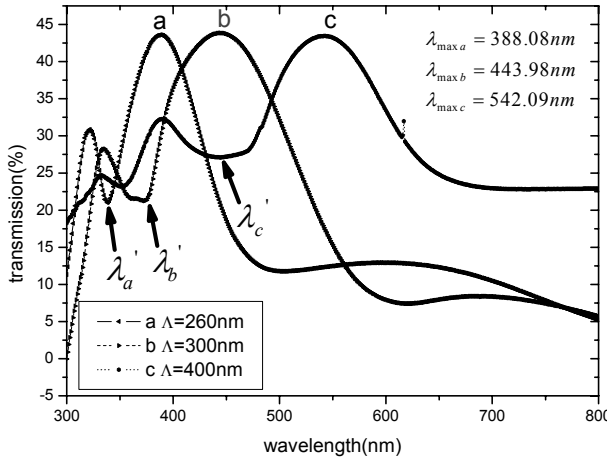

Fig.6 Transmission spectrum of the Ag nanostuctures with different periods. The left narrow peaks are extra peak transmission generated from the hybrid particles.

In contrast, we listed the measured values and theoretically calculated values of the LSPR absorption peaks in table 1. It can be seen that the experimental results fit to the theoretical values within the acceptable tolerance. It illustrates that the resonant peak exists at the measured position of the absorption peak and the experimental data are reliable. The two transmission peaks in Fig.6 may be caused by coupling effect of the LSPR between the two nanostuctures with the same periods. It is reasonable to believe that using this type of nanosructures as nanobiosensors is better than the traditional LSPR method which has pure small Ag nanostuctures only. Higher sensitivity and selectivity for biosample detecting and sensing are possible for our hybrid nanostructures.

Table 1 Comparison of the absorption peaks location between and experimental results and calculated value

Absorption peaks location	Experimental (nm)	Calculated (nm)
E_a	338.22	338.4
E_b	372.97	371.14
E_c	444.05	440.26

4.2 Different refractive index materials around the Ag nanostuctures

In this experiment, different refractive index inorganic pastern was used to change the refractive index of medium around the Ag nanostructures. The max value of transmittance spectroscopy of the bare Ag nanostuctures was monitored after each functioning (see Fig. 7). First, the max value λ_{maxa} of the Ag nanostuctures was measured to be 388.08 nm (see Fig. 7, curve a). Then Ag nanostucture sample is prepared for sensing experiments. After that, inorganic pastern was rotated and coated on the Ag nanostuctures. The refractive index of the inorganic pastern is 1.5. The max value λ_{maxb} after pastern attachment (see Fig. 7, curve b) was measured to be 400.01 nm, corresponding to an ditional 11.93 nm redshift. In order to know the influence of different refractive index materials around the Ag nanostuctures on the transmittance spectrum of the Ag nanostuctures, inorganic pastern which refractive index of 1.7 was spin coated on the Ag nanostuctures. After this function, the max value λ_{maxc} (see Fig. 7, curve c) was measured to be 412.08 nm, corresponding to a +12.07 nm shift. Meanwhile, the LSPR resonant peaks (also called absorption peaks) are denoted by λ_a', λ_b' and λ_c' which are 333.38nm, 341.03nm and 350.39nm respectively. It should be noted that different refractive index materials around the Ag nanostuctures have produced different transmittance spectrum shifts. The larger the refractive index, the larger peak transmission shift and bandwidth of the LSPR spectrum are, as shown in Fig. 7. Moreover, there are some sharp and smaller wave peaks besides the traditional transmittance peaks. These sharp peaks can be used as labels and the max value λ_{max} shifts of the biochemistrysensor are showed by the other transmittance peaks. This effect of enhancing the plasmon absorption by using a higher dielectric constant surrounding medium forms the basis of what is known as immersion spectroscopy.[13]

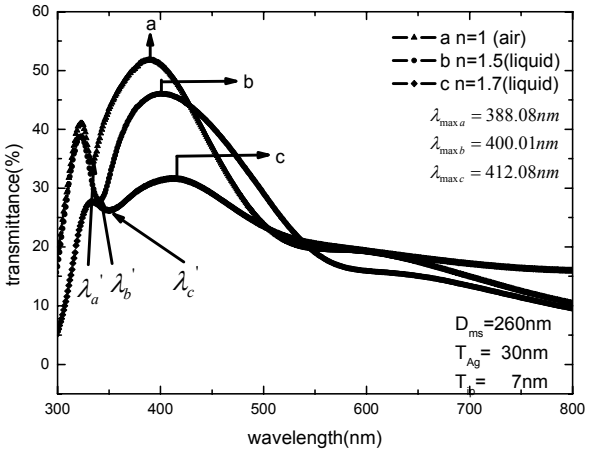

Fig7. Transmission spectrum of the Ag nanostuctures surrounding with the different refractive index materials. The left narrow peaks are extra peak transmission generated from the hybrid particles.

In contrast, we listed the measured values and theoretically calculated values of the LSPR absorption peaks in Table 2. It can be seen that the experimental results fit to the theoretical values within the acceptable tolerance. It illustrates that the resonant peak exists at the measured position of the absorption peak and the experimental data are reliable. Since the hybrid metal structure which is composed of two types of nanoprofiles has a definite period and it will generate a resonant peak caused by LSPR that is corresponding to the period, the theoretical calculation can be used to design a proper structure in the wavelength range of 300–800 nm. Well, we basically believe that the two transmission peaks shown in Fig. 7 are mainly caused by the coupling effect coming from different sizes and separated gaps of the two nanostuctures in one period. It is believed that the transmission peaks can be further modified through parameter adjustment of the hybrid structures. It is obvious that using hybrid nanosructures as nanobiosensors will have a higher sensitivity and selectivity for biosample detecting and sensing compared to the traditional LSPR method which has a single type of Ag nanostuctures only.

Table 2 Comparison of the absorption peaks location between and experimental results and calculated value

Absorption peaks location	Experimental (nm)	Calculated (nm)
E_a	333.38	338.4
E_b	341.03	348.50
E_c	350.39	357.8

5. CONCLUSIONS

We have developed a biochemistry nanosensor with hybrid Ag nanostuctures. The hybrid metallic nanostructure can excite the LSPR and be sensitive to metallic periods and the different refractive index materials around the Ag nanostuctures. We measured the transmittance spectrum of the hybrid nanostuctures, and found that there are some sharp and smaller wave peaks besides the traditional transmittance peaks. These sharp and smaller wave peaks can be used as the labels, meanwhile, the max value λ_{max} shifts of the biochemistrysensor are showed by the other transmittance peaks. In addition, compared with the conventional nanostuctures fabricated using sputtering, deposition, and chemical methods,[12] our hybrid nanostuctures have the advantages of controllable dimension, density and uniformity. It is reasonable to believe that the structure is possible to be used as a nanobiosensor. Biological molecules will be easily attached to the nanostructure. As the transmittance spectrum has a sharp and smaller wave peak, its sensitivity can be improved greatly.

ACKNOWLEDGMENT

The work was supported by 973 Program of China（No.2006CB302900) and the innovation foundation of Chinese Academy of science. Authors would like to thank, Miss Lifang Shi and Mr.Huan Yang for their kind contribution for the work.

REFERENCES

[1] G. P. Hicks, and S. J. Updike, "The preparation and characterization of lyophilized polyacrylamide enzyme gels for chemical analysis," *Anal. Chem.* **38**, 726-730 (1966).

[2] S. Link and M. El-Sayed, "Spectral properties and relaxation dynamics of surface plasmon electronic oscillations in gold and silver nanodots and nanorods," *J. Phys. Chem. B* **103**, 8410–8426 (1999).

[3] K. L. Kelly, E. Coronado, L. L. Zhao and G. C. Schatz, "The optical properties of metal nanostuctures: The influence of size, shape, and dielectric environment, *J. Phys. Chem. B* **107**, 668–677, 2003.

[4] S. Link and M. A. El-Sayed, "Optical properties and ultrafast dynamics of metallic nanocrystals," *Annu. Rev. Phys. Chem.* **54**, 331–366 (2003).

[5] J. B. Jackson and N. J. Halas, "Silver nanoshells: Variation in morphologies and optical properties," *J. Phys. Chem. B* **105**, 2743–2746 (2001).

[6] M. D. Malinsky, K. L. Kelly, G. C. Schatz and R. P. Van Duyne, "Chain length dependence and sensing capabilities of the localized surface plasmon resonance of silver nanostuctures chemically modified with alkanethiol self-assembled monolayers," *J. Am. Chem. Soc.* **123**, 1471–1482(2001).

[7] A. J. Haes and R. P. Van Duyne, "A nanoscale optical biosensor: sensitivity and selectivity of an approach based on the localized surface plasmon resonance spectroscopy of pyramidal silver nanostuctures," *J. Am. Chem. Soc.* **124**, 10596–10604 (2002).

[8] A. J. Haes and R. P. Van Duyne, "Nanosensors enable portable detectors for environmental and medical applications," *Laser Focus World* **39**, 153–156 (2003).

[9] J. C. Riboh, A. J. Haes, A. D. McFarland, C. R. Yonzon and R. P. Van Duyne, "A nanoscale optical biosensor: real-time immunoassay in physiological buffer enabled by improved nanostucture adhesion," *J. Phys. Chem. B* **107**, 1772–1780 (2003).

[10] A. J. Haes, S. Zou, G. C. Schatz and R. P. Van Duyne, "A nanoscale optical biosensor: The long range distance dependence of the localized surface plasmon resonance of noble metal nanostuctures," *J. Phys. Chem. B* **108**, 109–116 (2004).

[11] S. L. Zhu, X G. Luo, C. L. Du, F. Li, S. Y. Yin, Q. L. Deng, and Y. Q. Fu, "Hybrid metallic nanoparticles for excitation of surface plasmon resonance," *J. Appl. Phys.* **101**, 064701-1–064701-5 (2007)

[12] E. D. Palik, *Handbook of Optical Constants of Solids*. Academic, New York, 1985

[13] Paras N. Prasad Edited, *Nanophotonics*, Wiley Interscience Publication, 2004, Chapter5.